An 11 cm, 500 MHz, Hybrid Birdcage with Improved Tuning Range

Jatin Kulkarni[1], Nathan Laws[1], John P. Staab[1], George Entzminger[1], James A. Goodman[2], Joel R. Garbow[2], and F. David Doty[1]

[1]Doty Scientific, Columbia, SC, USA [2] Washington University, St. Louis, MO, USA

Abstract

Hybrid (or bandpass) birdcages have been used for extending the range of large birdcages to higher frequencies, but previous designs have often resulted in (1) inadequate tuning range to accommodate the desired range of loads and/or (2) inhomogeneous modes being impractically close to the homogeneous mode. In this study, an 8-section high-pass-weighted hybrid design with two parallel rungs per section, reminiscent of the Crozier topology, was constructed and evaluated. The coil was tested with 50 mM saline cylindrical samples of varying sizes and could be tuned and matched with relative ease. A four-point-drive tune/match network was used to improve isolation between channels. Interesting effects due to dielectric resonance in large samples are discussed.

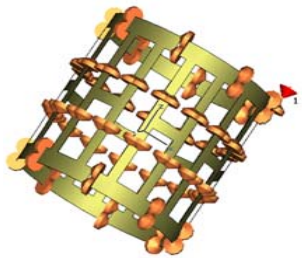

Figure 1 The 500 MHz Hybrid BirdCage coil as simulated in CST MWS. Some parts are hidden for better clarity. Capacitors are shown in this model as chamfered disks.

The Coil Structure

Figure 1 shows the coil geometry (sans external rf shield, sample, and matching elements) as simulated using full-wave EM software by Computer Simulation Technology (CST, Darmstadt, Germany), MWS 5.1. It consists of 8 sections with two parallel rungs per section. The capacitors, represented in the figure by chamfered disks, are connected between sections and also in series with the rungs to give a hybrid or bandpass configuration. At all locations, two parallel 1 kV ATC chip capacitors are used, one at each edge of the conductor foil, as shown. The rungs in each section are centrally shorted. The coil is fabricated from 0.06 mm copper foil on teflon substrate 0.5 mm thick and mounted on the outside of a polycarbonate coilform which is 1.5 mm thick. The coil diameter is 110 mm and the external slotted rf shield diameter is 142 mm. The end-ring is 11.25 mm wide and the inside distance between the end rings is 90 mm.

The Software

We carried out preliminary evaluations of three commercial electromagnetic simulation tools about 18 months ago before concluding that CST MWS 5.1 had a number of advantages for our mix of rf problems, which includes small-animal MRI rf coils, solids NMR spectroscopy rf coils, high-resolution NMR spectroscopy sample coils, and high-field MRI head coils. We also found its geometry construction tools and interface to be powerful and easy to use.

This CST code is based on a discretized solution of the integral formulation of Maxwell's equations; hence, the method is referred to as Finite Integration Technique (FIT). To solve these equations, a finite calculation domain is defined enclosing the application problem. A structured Cartesian mesh is created for half of the field equations (**E** and **B**), and a second Cartesian mesh, offset by half the element size in each direction from the first mesh, is created for the other half of the field equations (**H** and **D**). The use of two offset meshes greatly reduces discretization errors.

Finally, we note that a weakness of the software is the quality of the documentation for applications such as these, which can lead to a longer learning curve than would initially be expected from simple test cases. However, when the essential settings, options, methods, nomenclature, and techniques are properly understood, the software displays impressive versatility, power, and accuracy. Another current weakness is the time required for some runs which involve high Q structures containing small features. The subgridding feature is expected to be working more robustly within a few months, which should then permit much faster runs.

RF Circuit Model

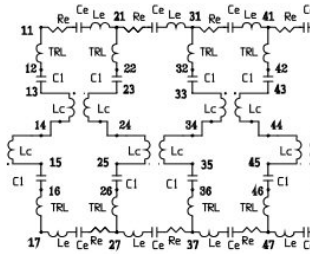

Figure 2 One-half (4 sections) of RF circuit model for an 8-section Hybrid BirdCage.

Figure 2 shows an rf circuit model for the 8-section Hybrid BirdCage coil. The model is somewhat better than one previously used in that the rungs are represented by a short transmission line at each end (TRL) with balanced couplings (L_C) between adjacent rungs. Most of the losses are represented by appropriate attenuation coefficients in the TRLs and series resistances (R_E) in the end ring segments (L_E) and tuning capacitors (C_E).

For circular polarization (CP) operation, coil symmetry is quite critical (especially for small coils) and sample detuning often exceeds the useful range of simple approaches.

Considerable improvement in coil symmetry and channel isolation is obtained by using a 4-point drive method. A simple method of doing this is to connect a low-loss half-lambda transmission line between nodes 17 and 57 and another between nodes 37 and 77 (not shown here). This sometimes brings in additional common modes near the homogeneous modes, but small inductors from the center points (quarter-lambda points) to ground on these phasing lines generally solve this problem.

Results

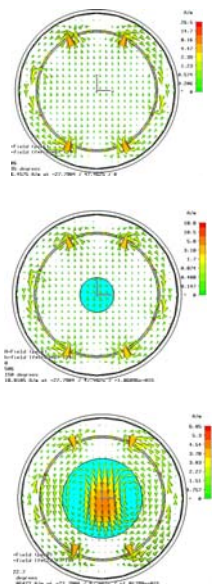

(From top to bottom) **Figure 3** Simulated H-field vector plot with **(a)** no load **(b)** small load and **(c)** large load. All cases were linearly excited.

Initially, the coil was simulated with cylindrical samples of varying diameters. For the sake of simplicity we will discuss the results for three cases: (a) Unloaded, (b) Small load (50 mM saline, diameter = 30 mm, length = 90 mm) and (c) Large load (50 mM saline, diameter = 70 mm, length = 90 mm). The instantaneous B_1 field vector plot at the z=0 plane for the unloaded case with linear excitation is depicted in **Figure 3(a)**. The B_1 homogeneity is quite good and is maintained even when we introduce the small load, as seen in **Figure 3(b)**. The most interesting effects are seen for the case of a large load, wherein the flux vectors are reversed in the center of the cylindrical sample (**Figure 3(c)**). The calculated mean circular polarization (CP) field (not shown here) shows similar strong central brightening and weak edge brightening, but with circular intensity profiles. This is not too surprising, since the sample dielectric resonance is dominating for heavily loaded cases and the asymmetries in the coil have relatively little effect. This is also in accordance with Tropp's analysis, which essentially states that all the coil can do for large samples at high fields is affect the length of the excited region. The homogeneity and S/N are then determined almost totally by the sample.

In addition to the flux reversal, the calculated main resonant mode shifted higher by 16.6 MHz for the large load case. This unusual increase was confirmed experimentally with a measured shift of 15.84 MHz. The tuning range for this coil exceeded 20 MHz and we were able to match these different loads, though the matching impedances were lower than expected.

Since the low-pass capacitors C_1 are quite large compared to the high-pass capacitors C_E, behavior is close to that of a high-pass birdcage, and we denote this coil a high-pass-weighted hybrid. It is largely because of this relationship that the nearest inhomogeneous modes were more than 75 MHz away from the main homogeneous mode. They may be moved farther away by connecting radially oriented capacitors from the mid-point of the rungs to the external shield. Experimentally, however, these were found to be unnecessary. **Figure 4** shows the simulated S11 plot obtained from CST MWS for the case with a small load.

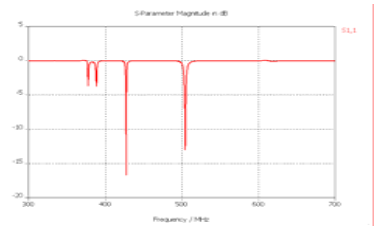

Figure 4 S11 plot, as simulated in CST MWS, showing the main homogeneous mode at 505 MHz and the nearest inhomogeneous mode at 428 MHz. A small load (50 mM saline, diameter = 30 mm, length = 90 mm) was used in this simulation.

Sample	C_E pF	C_1 pF	M_1 MHz (Expt)	Q_L @ m_1 (Expt)	M_1 MHz (Sim)	B_1 µT (Sim)
Unloaded	3.46	82	500	128	506	4.76
Small	3.46	82	500.15	108.5	505	7.82
Large	3.46	82	515.84	38.5	522.7	5.78

Small - Cylinder of diameter 30 mm, length 90 mm, centered, salinity=50mM

Large - Cylinder of diameter 70 mm, length 90 mm, centered, salinity=50mM

Table 1 shows some experimental data for the coil and also summarizes some simulated results for these cases, including central B_1 in µT for 0.5 W excitation, from CST MWS 5.1. (Note that the NMR-effective B_1, as listed, is one-half the peak field calculated for linear polarization, as linear polarization is equivalent to the sum of two oppositely rotating circular polarization fields, one of which is rotating in the wrong direction to induce NMR precession.) For consistency with recent trends we are reporting the matched Q of the resonator (including the sample and all losses), Q_L, which is half the isolated Q, Q_0, that has more often been used in NMR SNR analyses. Interestingly the simulated B_1 field with the small saline load is about 65% higher than that for the unloaded case, whereas with the large saline load it is 20% higher than that for the unloaded case. The simulations indicated the coil retained good symmetry over the tunable range, but experimental symmetry was, at least initially, less than expected.

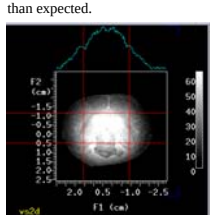

Figure 5 A fixed baboon brain image using a fast spin echo sequence.

Images were acquired from this coil at Washington University. **Figure 5** shows the image of a baboon brain collected using a fast spin echo sequence. Central brightening due to dielectric resonance effects of are clearly evident in this image.

Conclusions

The high accuracy of the CST MWS 5.1 code in predicting the mode frequencies and B1 from a physically accurate model of the coil provides a very high level of confidence in its calculated fields and rf efficiencies – hence, S/N.

An improved tuning range is obtained with good channel isolation using this 8-section hybrid design with 4-point drive. For heavy loads, the dielectric resonance effect dominates, resulting in central brightening in the image. The somewhat asymmetrical experimental intensity for the heavily loaded case is not yet understood, and the impedance transformations in the matching network also require further study.

REFERENCES

1. James Tropp, "Image Brightening in Samples of High Dielectric Constant:, *Journ. of Magn. Reson.*, 167, 12-24, 2004.
2. S. Crozier, D. M. Doddrell, US Pat #5,642,048, 1997.

Acknowledgements: This work supported by NIH R44 EB000445-03.